J. Biochem. 121, 854-861 (1997)

Expression of the Long Arm Sequence of Mouse Laminin $\alpha 1$, $\beta 1$, or $\gamma 1$ Chain in COS1 Cells and Assembly of Monkey-Mouse Hybrid Laminin

Tomoaki Niimi,* Kiyoshi Miki,*,† and Yasuo Kitagawa*,†,[1]

*Graduate Program of Biochemical Regulation, School of Agricultural Sciences, Nagoya University, and †Nagoya University BioScience Center, Furo-cho, Chikusa-ku, Nagoya 464-01

Received for publication, November 18, 1996

Mouse laminin $\alpha 1$, $\beta 1$, or $\gamma 1$ sequence covering truncated regions of the long arm was transiently expressed in monkey COS1 cells. Unlike natural laminins, in which only $\alpha\beta\gamma$ trimers are selectively assembled and disulfide-bonded at the long arm, a large fraction of mouse chains formed disulfide-bonded homopolymers. However, a small fraction of mouse $\beta 1$ (or $\gamma 1$) formed hybrid $\beta 1\gamma 1$ dimers with endogenous monkey $\gamma 1$ (or $\beta 1$). These hybrid $\beta 1\gamma 1$ dimers formed $\alpha 1\beta 1\gamma 1$ trimer with monkey $\alpha 1$. Mouse $\alpha 1$ also formed disulfide bonds with monkey $\beta 1\gamma 1$ dimer. Thus, a common mechanism is shared by laminin chains of different animal origins. Sequences in the E8 region at the C-terminal end of the long arm were crucial for this chain-selective assembly. When the C-terminal sequence of mouse $\beta 1$ long arm was extended beyond the α-loop, the hybrid trimer formation was diminished. This supported the model of altered chain arrangement around the α-loop.

Key words: basement membrane, coiled-coil, disulfide-bonding, heptad motif, laminin.

Laminins constitute a family of basement membrane glycoproteins which affect tissue morphogenesis by their effects on proliferation, migration, and differentiation of various types of cells (*1-4*). The best studied Engelbreth Holm Swarm (EHS) tumor isoform (laminin 1) is composed of $\alpha 1$ (400 kDa), $\beta 1$ (220 kDa), and $\gamma 1$ (210 kDa) chains, assembled and disulfide-bonded in a cross-shaped structure with three short arms and one rod-like long arm (*5-7*). The long arm is the site of chain assembly (*5-19*). It has many repeats of a heptad motif which form a hydrophobic surface along the α-helix with two charged edges at each side (*20-22*). Interchain hydrophobic interactions at this surface drive chain assembly, and ionic interactions at the edges determine chain selectivity. Since only $\alpha\beta\gamma$ trimers with same N- to C-terminus orientation are selectively formed, the intracellular assembly of laminin chains is a highly controlled process.

Several tissue-specific laminin isoforms composed of α, β, and γ variants have been reported (*23-27*). They share a common mechanism of assembly to produce the variety of chain compositions. For example, replacement of the $\alpha 1$ of a $\alpha 1\beta 1\gamma 1$ trimer (laminin 1) by $\alpha 2$ produces muscle membrane laminin (laminin 2) (*28-30*) while replacement of $\beta 1$ by $\beta 2$ results in a synaptic laminin (laminin 3) (*31*). Similar replacement is suggested in kalinin (laminin 5) and K-laminin (laminin 6), which have the chain compositions $\alpha 3\beta 3\gamma 2$ and $\alpha 3\beta 1\gamma 1$, respectively (*32, 33*). In 3T3-L1 adipocytes and endothelial cells, we found a laminin isoform ($\alpha x\beta 1\gamma 1$) in which $\alpha 1$ in laminin 1 is replaced by a smaller variant (αx) (*34, 35*).

By denaturation and renaturation of proteolytic fragments of laminin 1, Engel and coworkers showed that E8 fragments of three chains, which correspond to the C-terminal end of the long arm, mimic normal intracellular assembly (*36, 37*). By preparing recombinant or synthetic peptides comprising of mouse $\alpha 1$, $\beta 1$, and $\gamma 1$ partial sequences, Yamada and coworkers (*38-41*) showed that chain selection is controlled by defined sites at the C-terminal end of the long arm. Despite these *in vitro* data, we cannot answer the following questions: (1) Are the heptad motifs in the long arm of each chain sufficient for selective assembly? (2) What is the role of interchain disulfide-bond formation at the C- and N-termini of the long arm? (3) Do *in vitro* experiments reflect the microenvironment of intracellular chain assembly?

In this study, we expressed mouse $\alpha 1$, $\beta 1$, or $\gamma 1$ sequence covering various regions of the long arm in monkey kidney cells (COS1 cells) and detected monkey-mouse hybrid laminin with correct chain selection. Despite this selective assembly, however, most of the overexpressed recombinant laminin chains preferentially formed disulfide-bonded homopolymers. Since such homopolymers have not been observed in the natural process, we show here that the long arm region is not sufficient for the production of *bona fide* laminins.

MATERIALS AND METHODS

Plasmid Construction—Figure 1A summarizes the domains of mouse laminin 1 chains expressed in the cells. All plasmids are based on pEFneoER (*42*), which has erythropoietin receptor (ER) cDNA under the control of elonga-

[1] To whom correspondence should be addressed. Phone: +81-52-789-5227, Fax: +81-52-789-5228, e-mail: i45073a@nucc.cc.nagoya-u.ac.jp

Abbreviations: DMEM, Dulbecco's modified Eagle's medium; EF, elongation factor; EHS tumor, Engelbreth Holm Swarm tumor; ER, erythropoietin receptor; FCS, fetal calf serum; PCR, polymerase chain reaction; PMSF, phenylmethylsulfonyl fluoride; RT-PCR, reverse transcription-PCR.

tion factor (EF)-1α promoter (Fig. 1B). To utilize signal sequence of ER for insertion of partial laminin chains into endoplasmic reticulum, the ER cDNA fragment in pEFneoER was replaced by laminin cDNA fragments at the *Sma*I (or *Bam*HI) and *Eco*RI (or *Eco*RV) sites. To create a *c-myc* epitope tagging (*43*) and a termination codon at the 3′-end of laminin cDNA, two oligonucleotides with sequences of 5′ATCGAACAAAAGCTTATTTCTGAAGAAGACTTGTAGATGCA3′ and 5′TCTACAAGTCTTCTTCAGAAATAAGCTTTTGTTCGAT3′ were annealed and inserted into the *Bam*HI and *Nsi*I sites of pEFneoER. For the construction of pEFβ1ΔN1, a cDNA fragment corresponding to β1 sequence (*18*) from 1540 to 1765 amino acid residues was prepared by polymerase chain reaction (PCR) using pLAM (*44*) as a template and two primers with sequence of 5′GCTGGATCCGCTTGCAGCAGAGTGCAGCTGA3′ and 5′CGCGAATTCGCTAAGCAGGTGCTGTAAAACCG3′. The ER cDNA fragment in pEFneoER was replaced by this fragment at the *Bam*HI and *Eco*RI sites. For the construction of pEFβ1ΔN2 and pEFβ1ΔN3 having β1 sequence from 1424 to 1765 and from 1337 to 1765 amino acid residues, respectively, the 5′-ends of *Nco*I-*Cla*I and *Bgl*II-*Cla*I fragments from pLAM were connected to *Bam*HI linkers and these fragments were inserted between the *Bam*HI and *Cla*I sites of pEFβ1ΔN1. For the construction of pEFβ1ΔN4, a cDNA fragment corresponding to β1 sequence from 1157 to 1765 amino acid residues was prepared by PCR using pLAM and two primers with sequence of 5′GCTGGATCCCACCCTGCCACCAGTGCTTTGC3′ and 5′CGCGAATTCGCTAAGCAGGTGCTGTAAACCG3′, and the ER cDNA fragment in pEFneoER was replaced by this fragment at the *Bam*HI and *Eco*RI sites. To construct pEFβ1ΔN5 containing β1 sequence from 953 to 1765 amino acid residues, the *Hinc*II-*Cla*I fragment of pLAM was inserted between the *Sma*I and *Cla*I sites of pEFβ1ΔN1. A pEFβ1ΔNC1 encoding β1 sequence from 953 to 1699 amino acid residues was constructed by digestion and self-ligation of pEFβ1ΔN5. To construct pEFγ1ΔN1, a cDNA fragment corresponding to γ1 sequence (*17*) from 1329 to 1575 amino acid residues was prepared by reverse transcription (RT)-PCR using total RNA extracted from visceral endoderm-like F9 cells (*45*) as a template and two primers with sequence of 5′GCGGGATCCCCAATGACATTCTCAACAAC3′ and 5′GCAGATATCGGGCTTCTCGATAGACGGGG3′, and the ER cDNA fragment in pEFneoER was replaced by this fragment at the *Bam*HI and *Eco*RV sites. pEFγ1ΔN2 having the sequence from 996-1575 amino acid residues was constructed similarly, but two primers with sequence of 5′ GCAGGATCCAGGAGTGTCCGGCTTGTTAC3′ and 5′ GCAGATATCGGGCTTCTCGATAGACGGGG3′ were used for RT-PCR. To construct pEFα1ΔNC1 containing α1 sequence (*19*) from 1323 to 1777 amino acid residues, the 5′-end of the *Nco*I-*Eco*RI fragment from p1284 (provided by Dr. Y. Yamada) was connected to *Bam*HI linker, and the ER cDNA fragment in pEFneoER was replaced by this fragment at the *Bam*HI and *Eco*RI sites. For the construction of pEFα1ΔNC2 containing α1 sequence from 1323 to 2175 amino acid residues, the *Sph*I fragment from 5158 to 5696 nucleotide (nt) of α1 cDNA sequence was prepared by RT-PCR using two oligonucleotides of 5′GCGCGTAAAGATTTCCAGCC3′ and 5′GTCTCTGTCCAAAGCTCCTG3′ as primers and ligated to the *Sph*I site in pEFα1ΔNC1. The *Sph*I-*Eco*RI fragment from p1238 (provided by Dr. Y. Yamada) encoding from 5696 to 6641 nt of α1 cDNA was further inserted between the *Sph*I-*Eco*RI sites of this plasmid.

Cell Culture and Transfection—COS1 cells were maintained with Dulbecco's modified Eagle's medium (DMEM; Nissui Pharmaceutical) containing 10% fetal calf serum (FCS, Gibco Laboratories), 50 units/ml penicillin, 50 mg/ml streptomycin at 37°C under a humidified atmosphere of 5% CO_2. One day before transfection, the cells were plated to 60-mm dishes (Becton Dickinson) at a density of 3×10^5 cells/dish. Transfection was performed by calcium phosphate coprecipitation (*46*) using 20 μg/dish plasmids. After 4 h, DNA precipitate was washed off from the cultures and the cells were fed with DMEM containing 10% FCS. The cells were then re-plated to 35-mm dishes one day after transfection, and labeled the next day.

Cell Labeling and Immunoprecipitation—The transfected COS1 cells were labeled with 600 μl of methionine-free Eagle's minimal essential medium (Sigma) containing 0.1 mCi/ml Tran^{35}S-label (ICN Radiochemical) for 4 h at 37°C. After removing the medium, the cells were lysed by adding 1,000 μl of a buffer containing 10 mM Tris-HCl (pH 7.4), 1 mM NaCl, 5 mM EDTA, 0.1% (w/v) sodium deoxycholate, 0.1% (w/v) SDS, and 1 mM phenylmethylsulfonyl fluoride (PMSF). Aliquots of cell lysate corresponding to 1.5×10^7 cpm of incorporated radioactivity into cellular proteins were diluted to 500 μl with the same buffer, and laminin chains were immunoprecipitated overnight at 4°C by mixing 1 μl of antiserum against mouse EHS laminin (*34, 35*). This antiserum immunoprecipitates $\alpha1\beta1\gamma1$ trimers of various origins and gives stronger signals of β1 and γ1 relative to α1 in the immunoblotting of mouse laminin-1. For the immunoprecipitation of recombinant laminin chains tagged with *c-myc* epitopes, the cells were lysed with a buffer containing 10 mM Tris-HCl (pH 7.4), 150 mM NaCl, 5 mM EDTA, 1% (v/v) NP-40, and 1 mM PMSF, cell lysate was diluted as above, and immunoprecipitated by mixing 5 μl of monoclonal antibody to *c-myc* (Cat # OP10 from Oncogene Science). Other details of the immunoprecipitation procedures were as described (*34, 35*).

SDS Gel Electrophoresis—One- and two-dimensional SDS gel electrophoreses under reducing and non-reducing conditions were carried out as described (*34, 35*), except that 3-10% (w/v) acrylamide was used for one-dimensional electrophoresis under reducing and non-reducing conditions. In two-dimensional electrophoresis, 4% (w/v) gel for the first dimension under non-reducing conditions, and 3-10% gel was used for the second dimension under reducing conditions. After fixation with a solution containing 10% (v/v) trichloroacetic acid, 30% (v/v) methanol, and 10% (v/v) acetic acid for 30 min, the gel was dried and analyzed with a Fuji Film BAS 2000 Image Analyzer.

RESULTS

Plasmids Encoding the Long Arm Domains of Mouse Laminin $\alpha1$, $\beta1$, and $\gamma1$—Figure 1A summarizes the plasmids constructed in this study to express various long arm sequences of mouse α1, β1, and γ1 in COS1 cells. To determine the critical region of β1 long arm for the assembly, we prepared the pEFβ1ΔN series covering β1 sequence extended from the C-terminal E8 region to the

N-terminal end of the short arm. Since *in vitro* experiments showed the importance of the C-terminal end, pEFβ1ΔNC1 was prepared in which the E8 region was truncated. pEFγ1ΔN1 and pEFγ1ΔN2 cover the C-terminal end and the whole of mouse γ1 long arm, respectively, while pEFα1ΔNC1 and pEFα1ΔNC2 cover the N-terminus and the whole of mouse α1 long arm, respectively. Mouse laminin has many cysteine residues for intrachain disulfide-bonding in the short arm region of α1, β1, and γ1, in domain G of α1 and in the α-loop of β1, but they are depleted in the long arm region (*17-19*). Through the limited number of cysteine residues in the long arm, β1 and

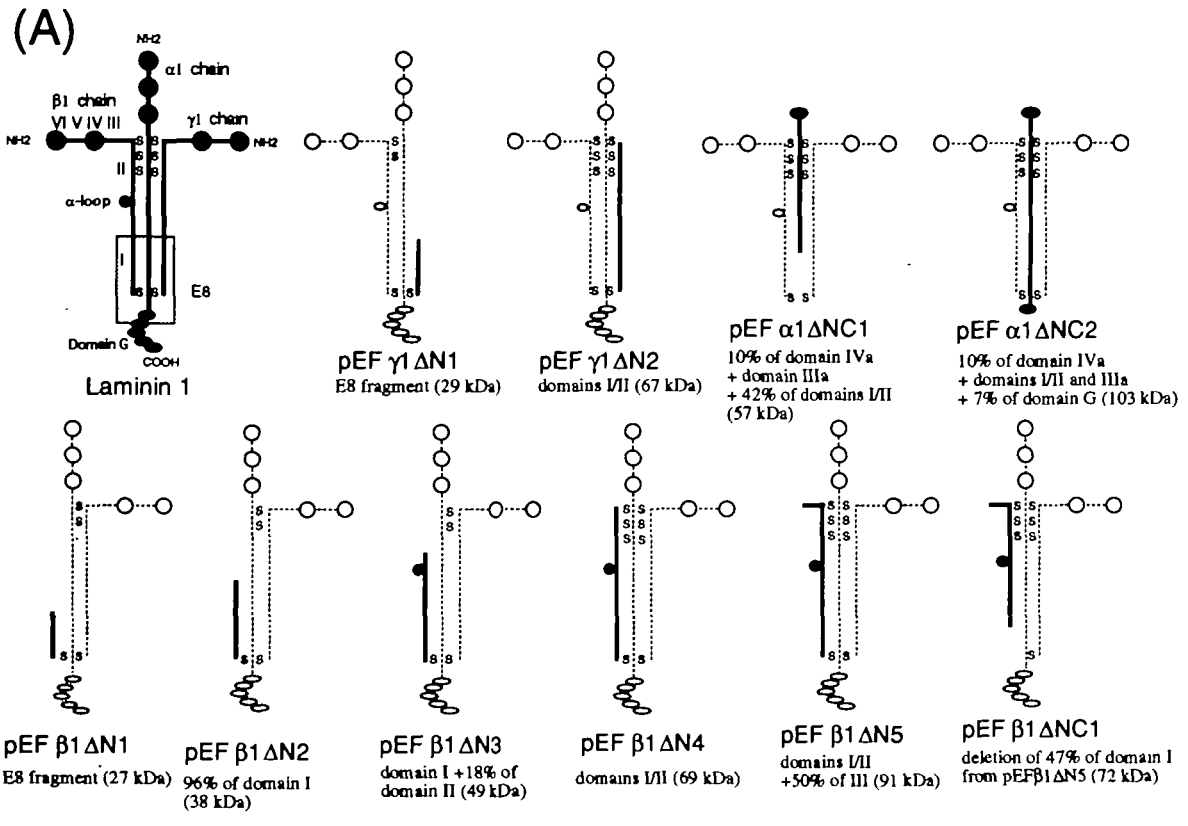

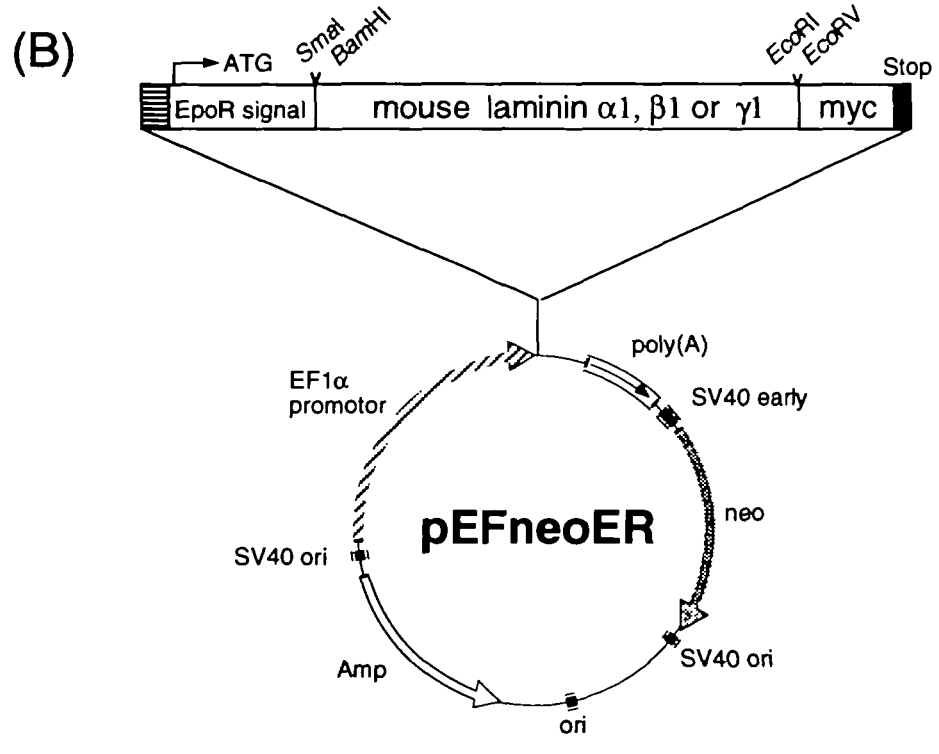

Fig. 1. **Plasmids encoding long arm regions of mouse α1, β1, and γ1 chain.** A: Simplified mouse laminin structure, its major domains, and cysteine residues for interchain disulfide-bonding (S) are shown at left top of the panel. The long arm sequences encoded by each plasmid are shown by thick lines, and other parts by dotted lines. Under the name of each plasmid, encoded sequences are briefly explained together with calculated molecular mass of the products. B: Map of pEFneoER and the strategy of plasmid construction are shown.

$\gamma 1$ are disulfide-bonded at the N- and C-termini, while $\alpha 1$ is disulfide-bonded to $\beta 1$ and $\gamma 1$ only at the N-terminus of the long arm. Since the process of chain assembly is followed by non-reducing and reducing SDS gel electrophoresis in this study, all constructs are designed to contain at least one cysteine residue for this interchain disulfide-bonding.

Expression of Mouse Laminin α1, β1, and γ1 in COS1 Cells—To detect the transient expression of mouse $\alpha 1$, $\beta 1$, and $\gamma 1$ chains in COS1 cells, the cells were labeled with [^{35}S]methionine/cysteine, and the cell lysate was immunoprecipitated with anti-myc monoclonal antibody two days after transfection with various plasmids. Endogenous monkey laminin chains were also immunoprecipitated with anti-EHS tumor laminin antibody from mock-transfected COS1 cells. As summarized in Fig. 2, SDS gel electrophoresis of immunoprecipitates under reducing conditions detected ectopic laminin chains whose migration was consistent with their calculated molecular mass (Fig. 1A). Despite many weak bands due to nonspecific precipitation of endogenous proteins, the identity of ectopic laminin chains was established by comparing their precipitates with the parallel immunoprecipitates from mock transfected COS1 cells with anti-myc monoclonal antibody (lane under anti-myc/None). Comparable density of the ectopic laminin bands confirms that the efficiency of transfection was normalized. However, no specific product was detected from cells transfected with pEFα1ΔNC1 and pEFα1-ΔNC2. Since anti-EHS tumor laminin antibody precipitated the expected products (see Figs. 3 and 4B), it appeared that the myc epitope at the C-terminus of the recombinant mouse $\alpha 1$ chain was not accessible to the antibody or had been clipped by endogenous protease(s). As indicated by open and filled arrowheads in Fig. 2, doublet bands were detected in most transfectants. Since a single band with faster migration was observed instead of the doublet bands in the presence of tunicamycin (not shown), we concluded that the doublet bands were due to different degrees of *N*-glycosylation. As described below, most of the recombinant products have the ability to form disulfide-bonded dimers or trimers with endogenous monkey laminin chains. Because of this interaction, the endogenous monkey laminin chains were co-immunoprecipitated with anti-myc antibody as indicated by arrows for $\gamma 1$ and $\beta 1$ in the pEFβ1ΔN5 and pEFγ1ΔN1 lanes, respectively.

Assembly of Monkey-Mouse Hybrid Laminins and Homopolymer Formation of Mouse Laminin α1, β1, and γ1—The assembly of ectopic mouse laminin chains with endogenous monkey laminin chains was analyzed by im-

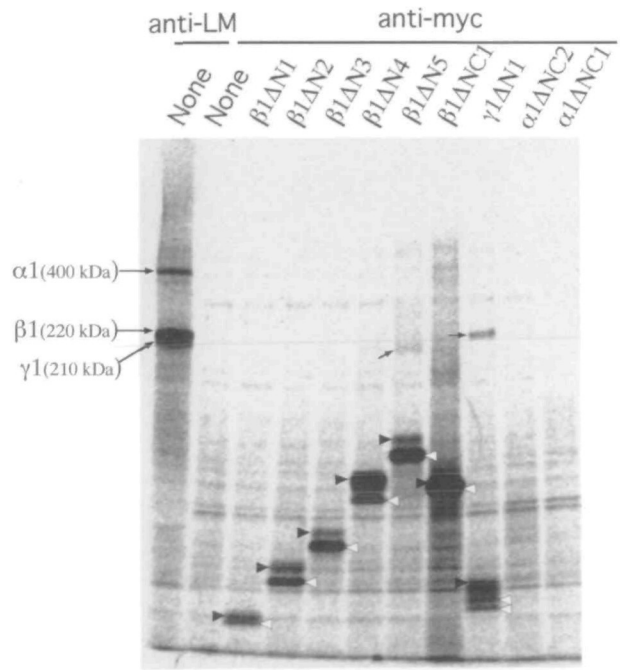

Fig. 2. **Reducing SDS gel electrophoresis of immunoprecipitates with anti-myc antibody from COS1 cells expressing mouse laminin chains.** COS1 cells transfected with indicated plasmids ("pEF" is omitted) were labeled with [^{35}S]methionine/cysteine, cell lysate was immunoprecipitated with anti-myc antibody and precipitates were separated by SDS gel electrophoresis under reducing conditions. Mock-transfected cells were also labeled and immunoprecipitated with anti-myc (lane under anti-myc/None) or with anti-EHS tumor laminin (lane under anti-LM/None) antibody. Arrows indicate the migration positions of endogenous monkey $\alpha 1$, $\beta 1$, and $\gamma 1$ chains. Filled and open arrowheads indicate the migration positions of ectopically expressed mouse laminin chains. In this electrophoresis, lysate from pEFγ1ΔN2-transfected cells is not analyzed, but separate electrophoresis showed comparable results to pEFγ1-ΔN1-transfected cells in terms of the migration distance consistent with calculated molecular mass, the doublet bands and the density of specific bands.

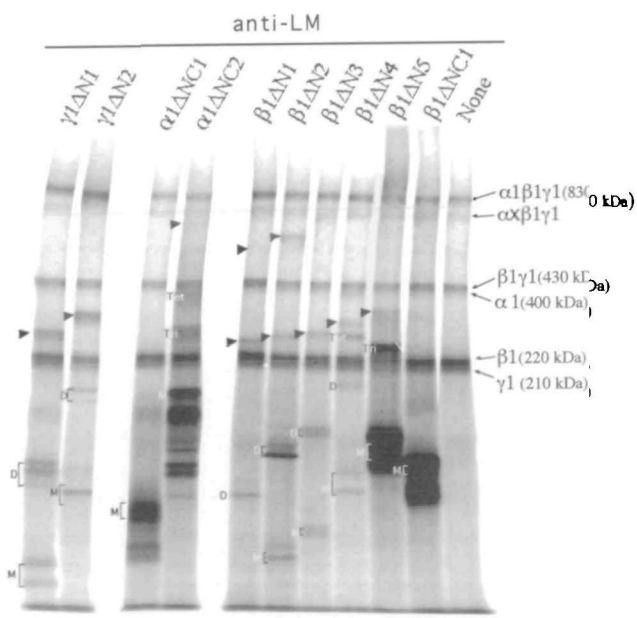

Fig. 3. **Non-reducing SDS gel electrophoresis of immunoprecipitates with anti-EHS tumor laminin antibody from COS1 cells expressing mouse laminin chains.** COS1 cells transfected with the indicated plasmids were labeled with [^{35}S]methionine/cysteine, cell lysate was immunoprecipitated with anti-EHS tumor laminin antibody and precipitates were separated by SDS electrophoresis under non-reducing conditions. Mock-transfected cells were also labeled and immunoprecipitated with the same antibody (None). Arrowheads indicate the migration positions of monkey-mouse hybrids. M, D, Tri, and Tet indicate the migration positions of the monomer, homodimer, homotrimer, and homotetramer of mouse chains, respectively. The migration distance of the indicated homopolymers was consistent with calculated molecular mass. Other details were the same as in Fig. 2.

munoprecipitation of metabolically labeled COS1 cells with anti-EHS tumor laminin antibody followed by SDS gel electrophoresis of the immunoprecipitates under non-reducing conditions where the interchain disulfide-bondings are preserved (Fig. 3). The chain composition of the complex was confirmed by two dimensional SDS gel electrophoresis, as summarized in Fig. 4, in which non-reducing electrophoresis in the first dimension (left to right) is followed by reducing electrophoresis in the second dimension (top to bottom). In this electrophoresis, monomeric proteins come to the diagonal while proteins disulfide-bonded to each other migrate below the diagonal, and form a vertical line for each disulfide-bonded complex. Since 4% and 3–10% acrylamide gels were used for the first and the second dimension, respectively, monomeric proteins smaller than 150 kDa were not separated in the first dimension and came to the vertical line in the lower right quadrant of the gel.

Endogenous monkey laminin chains: The lane None in Fig. 3, to which the cell lysate from mock-transfected COS1 cells was applied, shows two laminin trimers in addition to $\beta1\gamma1$ dimer, monomeric $\alpha1$, $\beta1$, and $\gamma1$. Two-dimensional electrophoresis in Fig. 4 confirms that one trimer was composed of $\alpha1$, $\beta1$, and $\gamma1$ chains, while the other had a smaller α variant chain (tentatively referred to as αx) instead of the $\alpha1$ chain. Since $\beta1\gamma1$ was the only dimer of monkey laminin chains observed in Fig. 3 and Fig. 4, we can conclude that $\beta1$ and $\gamma1$ were first disulfide-bonded to form a $\beta1\gamma1$ dimer, then $\alpha1$ or αx joined it to form $\alpha1\beta1\gamma1$ or $\alpha x\beta1\gamma1$ trimer. Such chain composition and the assembly process of monkey laminin chains in COS1 cells are strikingly similar to those we reported for the laminin isoforms in endothelial cells (*34*). Given this information on endogenous laminin expression, we studied the behavior of recombinant mouse laminin chains by focusing on the bands which appeared specifically in transfectants.

Assembly of mouse laminin γ1 with monkey laminin β1: In Fig. 3, lanes pEF$\gamma1\Delta$N1 and pEF$\gamma1\Delta$N2 show a transfection-dependent band (indicated by arrowhead) which migrated between endogenous $\beta1/\gamma1$ monomer and the $\beta1\gamma1$ dimer. When the immunoprecipitates from pEF$\gamma1$-ΔN2-transfected cells were separated by two-dimensional

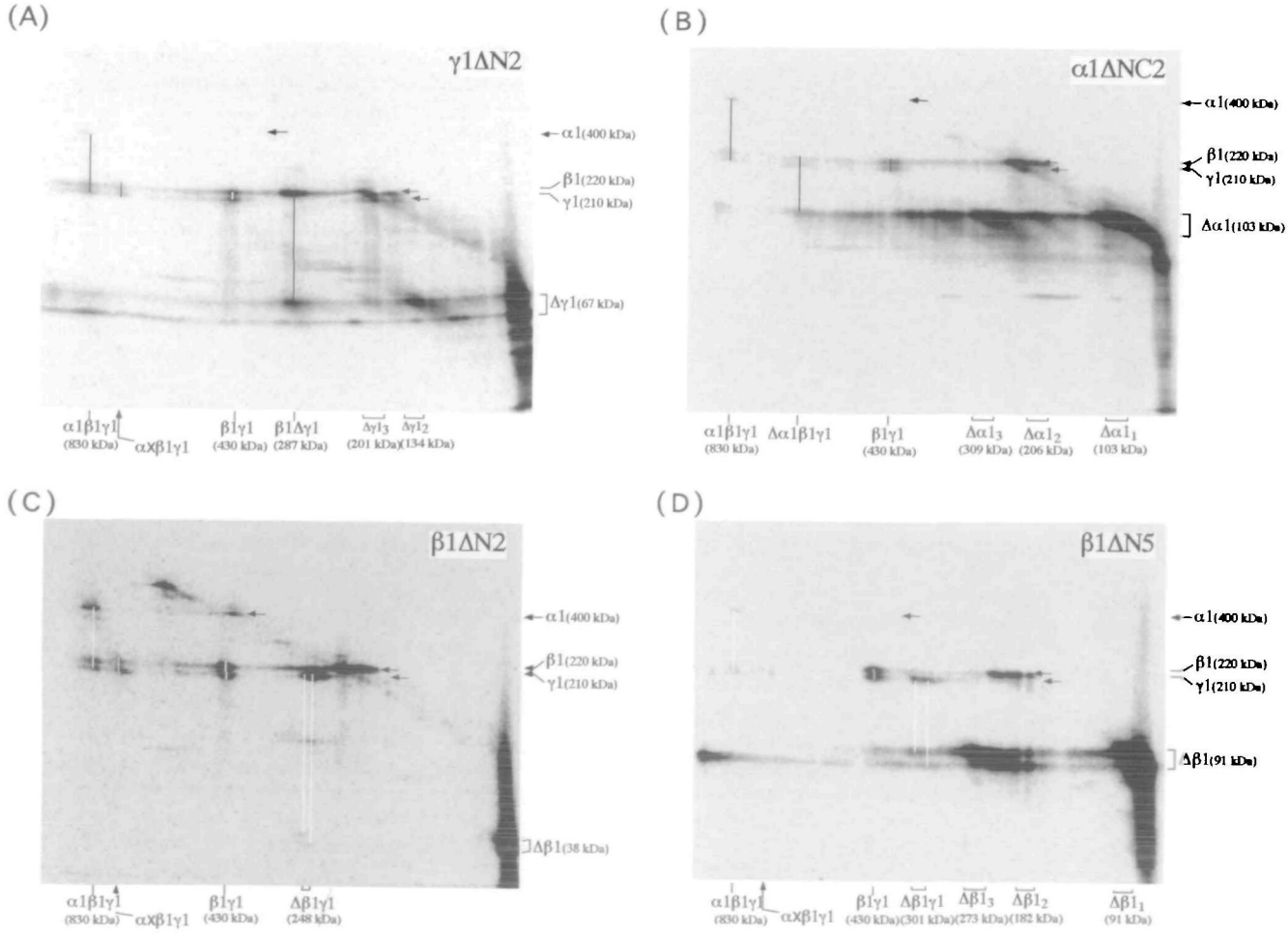

Fig. 4. **Two-dimensional electrophoresis of immunoprecipitates with anti-EHS tumor laminin antibody from COS1 cells expressing mouse laminin chains.** COS1 cells transfected with indicated plasmids were labeled with [^{35}S]methionine/cysteine, cell lysate was immunoprecipitated with anti-EHS tumor laminin antibody and precipitates were separated by SDS electrophoresis under non-reducing conditions in the first dimension (from left to right) followed by reducing conditions in the second dimension (from top to bottom). Migration positions of disulfide-bonded complexes in the first dimension and monomers in the second dimension are indicated at the bottom and right margins of each panel, respectively. $\Delta\alpha1$, $\Delta\beta1$, and $\Delta\gamma1$ indicate truncated mouse laminin chains. Vertical lines are drawn to connects spots which co-migrated in the first dimension due to disulfide-bonding to each other.

SDS gel electrophoresis (Fig. 4A), the band was separated into two spots aligned on the vertical line indicated as $\beta1\Delta\gamma1$ at the bottom. Since the migration distance in the second dimension confirmed that these spots are the monkey $\beta1$ chain and the mouse recombinant $\gamma1$ chains, we conclude that the long arm of mouse $\gamma1$ can selectively interact with monkey $\beta1$ to form disulfide-bonded hybrid $\beta1\Delta\gamma1$ dimer. The $\beta1\Delta\gamma1$ band produced by pEF$\gamma1\Delta$N1 (Fig. 3) gave essentially the same pattern of two-dimensional electrophoresis (not shown). Thus, the C-terminal half of domain I (Fig. 1A) is sufficient to allow mouse $\gamma1$ chain to assemble with monkey $\beta1$ chain. Despite the formation of the hybrid $\beta1\Delta\gamma1$ dimer, further assembly of monkey $\alpha1$ chain to form the disulfide-bonded $\alpha1\beta1\Delta\gamma1$ trimer was not detected even for the construct covering the entire long arm (pEF$\gamma1\Delta$N2). This suggests that the homology between monkey and mouse $\gamma1$ sequences is too low to support this interactions or that the short arm of $\gamma1$ is needed for the $\alpha\beta\gamma$ trimer assembly.

In addition to $\beta1\Delta\gamma$ dimer and monomeric $\Delta\gamma$ (M), formation of disulfide-bonded homodimer of $\Delta\gamma$ (indicated with "D" in the pEF$\gamma1\Delta$N1 and pEF$\gamma1\Delta$N2 lanes in Fig. 3) was observed. Two-dimensional electrophoresis of a larger amount of radioactive immunoprecipitates from pEF$\gamma1$-ΔN2-transfected cells (Fig. 4A) showed the formation of homotrimer as well. Less glycosylated products of pEF$\gamma1$-ΔN2 tended to form even more complicated disulfide-bonded complexes aligned in a horizontal line (Fig. 4A). Since the endogenous laminin chains in the same sample did not show such homopolymer formation, we can exclude the possibility that the homopolymers of ectopic mouse laminin chains are artifacts due to oxidation during immunoprecipitation after lysis of the cells. Overexpression of single type of laminin chain or expression of sequences missing the short arm may be the reason for this uncontrolled assembly. SDS electrophoresis of the radiolabeled media showed that such inappropriate laminin complexes were secreted (not shown), probably through the default pathway.

Homopolymer formation of mouse laminin $\alpha1$: The long arm of mouse $\alpha1$ chain was found to be less active in complex formation with monkey $\beta1$ and $\gamma1$ chains. Most of the pEF$\alpha1\Delta$NC1 products, in which the C-terminal end of the long arm was truncated, remained as monomers (the pEF$\alpha1\Delta$NC1 lane in Fig. 3). When the entire long arm was expressed by pEF$\alpha1\Delta$NC2, most of the product formed homopolymers, and a very small amount was recruited for $\Delta\alpha1\beta1\gamma1$ hybrid formation (the pEF$\alpha1\Delta$NC2 lane in Fig. 3 and Fig. 4B). Augmentation of the reactivity of α chain by the addition of the C-terminal end of the long arm is consistent with the *in vitro* experiment by Utani *et al.* (*38, 39*), but our *in vivo* experiment shows that the self-association is also augmented. This suggests that the domain G next to the C-terminal end of the long arm might be important for prevention of self-association of the $\alpha1$ chain. Probably because the domain G was truncated, the products of pEF$\alpha1\Delta$NC1 and pEF$\alpha1\Delta$NC2 tended to be clipped at the C-termini into many smaller bands (the pEF$\alpha1\Delta$NC1 and pEF$\alpha1\Delta$NC2 lanes in Fig. 3).

Functional long arm domains of mouse laminin $\beta1$: To identify the functional domains of the mouse $\beta1$ long arm for chain assembly, we transfected COS1 cells with pEF$\beta1\Delta$N plasmids, which encode different lengths of the C-terminus of the mouse $\beta1$ long arm (Fig. 1A). As indicated by arrowheads in the pEF$\beta1\Delta$N1 lane in Fig. 3, the mouse $\beta1$E8 fragment formed disulfide-bonded $\Delta\beta1\gamma1$ dimer and $\alpha1\Delta\beta1\gamma1$ trimer. This ability was augmented in the product of pEF$\beta1\Delta$N2, in which the sequence extended to the α-loop. Two-dimensional electrophoresis of immunoprecipitates from the pEF$\beta1\Delta$N2-transfected cells in Fig. 4C suggested that two forms of mouse $\Delta\beta1$ chain at different stages of glycosylation selectively interacted with monkey $\gamma1$ chain for the formation of $\Delta\beta1\gamma1$ dimer, but the amount of mouse $\Delta\beta1$ chain recruited for $\alpha1\Delta\beta1\gamma1$ trimer formation was too small to be detected. When the mouse $\beta1$ sequence was extended beyond the α-loop, on the other hand, the $\alpha1\Delta\beta1\gamma1$ trimer formation was lost and the $\Delta\beta1\gamma1$ dimer was gradually diminished (the pEF$\beta1$-ΔN3, pEF$\beta1\Delta$N4, and pEF$\beta1\Delta$N4 lanes in Fig. 3). This apparently conflicting result suggests a crucial role of the α-loop for chain assembly. When the E8 region was truncated from the mouse $\beta1$ long arm sequence (the pEF$\beta1\Delta$NC1 lane in Fig. 3), complex formation was completely lost and the product remained as the monomer. Recombinant mouse $\beta1$ chains also formed homopolymers, as did $\gamma1$ and $\alpha1$ chains. Two-dimensional electrophoresis of immunoprecipitates from pEF$\beta1\Delta$N5 transfected cells (Fig. 4D) showed the formation of disulfide-bonded homopolymers. The less glycosylated form tended to form an even more complicated complex aligned in a horizontal line.

DISCUSSION

To explore the possibility of manipulating the *in vivo* process of laminin chain assembly, we expressed truncated long arm regions of mouse $\alpha1$, $\beta1$, or $\gamma1$ chain in monkey COS1 cells. Since a transient expression system was employed for this purpose, there is no doubt but that the population of COS1 cells expressing recombinant products was limited. This implies that a significant part of monkey laminin chains had no chance to interact with their mouse counterparts. Nevertheless, we were able to detect chain-selective disulfide-bonding of correct pairs such as mouse $\beta1$ and monkey $\gamma1$ chains, mouse $\gamma1$ and monkey $\beta1$ chains, mouse $\alpha1$ chain, and monkey $\beta1\gamma1$ dimer, and mouse $\beta1$-monkey $\gamma1$ dimer and monkey $\alpha1$ chain. No pairing between $\alpha1$s, $\beta1$s, and $\gamma1$s of different origins was detected. Mouse chains assembled with monkey chains in the right order, with the $\beta\gamma$ dimer being formed first and the α chain attaching next to form the $\alpha\beta\gamma$ trimer (*34, 35, 47*). Neither $\alpha1$ chain interacts directly with $\beta1$s or $\gamma1$s of either origin. Thus, our results open the door to producing hybrid laminins composed of α, β, and γ chains from different animal origins.

Five α variants, three β variants and two γ variants have been cloned from mouse and human (*23-27*). Their long arm sequences are varied but all have a well-aligned heptad motif with hydrophobic residues at the first and fourth positions and charged residues at the fifth and seventh positions. This motif creates a hydrophobic surface along the α-helix with two charged edges at each side. Interchain hydrophobic interactions at this surface drive the chain assembly and ionic interactions at the edges determine the chain selectivity (*20-22*). These facts suggest that laminin chains share a common mechanism of assembly to produce chains of various compositions. Although theoretically there are 30 possible combinations of laminin αs ($\alpha1$, $\alpha2$,

α3, α4, and α5), βs (β1, β2, and β3) and γs (γ1 and γ2) to form $\alpha\beta\gamma$ trimers, only 8 combinations (laminin 1 through laminin 8) have been found in nature (*48*). This implies that the types of laminin chains expressed in differentiated tissue cells are limited and laminin chains cannot interact in all possible combinations. Our results of hybrid laminin formation showed the future direction for producing novel laminin isoforms with undiscovered chain compositions.

Despite the chain-selective hybrid formation, a large fraction of ectopic laminin chains were disulfide-bonded to form homopolymers. Since such homopolymers have not been found among natural laminins, the process observed in COS1 cells was obviously out of control. This could be due to the overexpression of a single type of laminin chain in a limited sub-population of COS1 cells. However, compared with the high level of laminin synthesized in embryonal carcinoma F9 cells (*45*), for example, the expression in COS1 cells could not be considered excessive. If we assume that a supporting machinery such as molecular chaperones, supports the laminin chain assembly, however, relative overexpression of a single type of recombinant chain in excess of the "capacity" of poor laminin-producing cells like COS1 could lead to uncontrolled chain assembly.

The homodimer formation, at the same time, revealed that disulfide-bonding between laminin chains is a rapid reaction which fixes even unfavorable pairs before the constituent chains can dissociate for another round of association. This implies that protein disulfide isomerase present in endoplasmic reticulum produces a environment different from that in the *in vitro* systems in which the domains and amino acid sequence for the laminin chain assembly have been analyzed (*36-41*). Our *in vivo* results showed that the control of rapid disulfide-bonding will be an important issue to be overcome in the future design of "artificial laminins."

Truncation of the long arm sequences has confirmed the crucial role of the E8 region in the *in vivo* laminin chain assembly. This region of mouse β1 and γ1 chains was able to form hybrids with monkey γ1 and β1. Moreover, deletion of this domain from mouse α1 and β1 chains diminished the hybrid formation. These results are consistent with the *in vitro* observations made by Engel and coworkers using proteolytic fragments (*36, 37*) and by Yamada and coworkers using recombinant of synthetic peptides (*38-41*). A surprising result of the *in vivo* experiments was that deletion of the E8 region diminishes homopolymer formation as well.

Another interesting observation made only the in *in vivo* system was that the ability of β1 to form a hybrid trimer is lost when its sequence was extended beyond the α-loop. The α-loop is a domain found only in laminin βs (see Fig. 1A), where the repeats of the heptad motif are interrupted and the sequence is looped out by intrachain disulfide-bondings. Electron microscopic observation of laminin 1 shows a bending of the long arm at this position (*5-7*). By scoring the interchain ionic interactions among laminin chains through their heptad motifs in the long arm, Beck *et al.* suggested that an anti-clockwise chain arrangement of α1-β1-γ1 when viewed from the N-terminus is most probable based on the reported C-terminal sequences up to the α-loop. However, the probability of the N-terminal half was increased when this chain order was altered around the α-loop (*20*). Our result of diminished hybrid trimer formation in the pEFβ1ΔN3 and pEFβ1ΔN4 transfectants also predicts this altered chain arrangement around the α-loop.

We thank Dr. Y. Yamada (National Institute of Dental Research, National Institute of Health, Bethesda, MD) for p1284 and p1238, Prof. R. Sasaki (Faculty of Agriculture, Kyoto University, Kyoto, Japan) for pEFneoER, Ms. C. Kumagai for technical assistance in SDS gel electrophoresis, Prof. A.M. Tartakoff (Case Western Research University, Cleveland OH) for proofreading the manuscript, and Dr. T. Kadowaki for comments on the manuscript.

REFERENCES

1. Martin, G.R., Timpl, R., and Kühn, K. (1988) Basement membrane proteins: molecular structure and function. *Adv. Protein Chem.* **39**, 1-50
2. Timpl, R. (1989) Structure and biological activity of basement membranes. *Eur. J. Biochem.* **180**, 487-502
3. Engel, J. (1992) Laminins and other strange proteins. *Biochemistry* **31**, 10633-10651
4. Beck, K., Hunter, I., and Engel, J. (1990) Structure and function of laminin: anatomy of a multidomain glycoprotein. *FASEB J.* **4**, 148-160
5. Burgeson, R.E., Chiquet, M., Deutzmann, R., Ekblom, P., Engel, J., Kleinman, H., Martin, G.R., Meneguzzi, G., Paulsson, M., Sanes, J., Timpl, R., Tryggvason, K., Yamada, Y., and Yurchenco, P.D. (1994) A new nomenclature for laminins. *Matrix Biol.* **14**, 209-211
6. Engel, J., Odermatt, E., Engel, A., Madri, J.A., Furthmayr, H., Rhode, H., and Timpl, R. (1981) Shapes, domain organization and flexibility of laminin and fibronectin, two multifunctional proteins of the extracellular matrix. *J. Mol. Biol.* **150**, 97-120
7. Engel, J. (1993) Structure and function of laminin in *Molecular and Cellular Aspects of Basement Membranes* (Rohrbach, D.H. and Timpl, R., eds.) pp. 147-176, Academic Press, San Diego
8. Paulsson, M., Deutzmann, R., Timpl, R., Dalzoppo, D., Odermatt, E., and Engel, J. (1985) Evidence for coiled-coil α-helical regions in the long arm of laminin. *EMBO J.* **4**, 309-316
9. Graf, J., Iwamoto, Y., Sasaki, M., Martin, G.R., Kleinman, H.K., Robey, F.A., and Yamada, Y. (1987) Identification of an amino acid sequence in laminin mediating cell attachment, chemotaxis, and receptor binding. *Cell* **48**, 989-996
10. Charonis, A.S., Skubitz, A.P., Kolialos, G.G., Reger, L.A., Dege, J., Vogel, A.M., Wohlhueter, R., and Furcht, L.T. (1988) A novel synthetic peptide from the B1 chain of laminin with heparin-binding and cell adhesion-promoting activities. *J. Cell Biol.* **107**, 1253-1260
11. Iwamoto, Y., Robey, F.A., Graf, J., Sasaki, M., Kleinman, H.K., Yamada, Y., and Martin, G.R. (1987) YIGSR, a specific laminin pentapeptide, inhibits experimental metastasis formation. *Science* **238**, 1132-1134
12. Tashiro, K., Sephel, G.C., Weeks, B., Sasaki, M., Martin, G.R., Kleinman, H.K., and Yamada, Y. (1989) A synthetic peptide containing the IKVAV sequence from the A chain of laminin mediates cell attachment, migration, and neurite outgrowth. *J. Biol. Chem.* **264**, 16174-16182
13. Schittny, J.C. and Yurchenco, P.D. (1990) Terminal short arm domains of basement membrane laminin are critical for its self-assembly. *J. Cell Biol.* **110**, 825-832
14. Sung, U., O'Rear, J.J., and Yurchenco, P.D. (1993) Cell and heparin binding in the distal long arm of laminin: identification of active and cryptic sites with recombinant and hybrid glycoprotein. *J. Cell Biol.* **123**, 1255-1268
15. Nomizu, M., Kim, W.H., Yamamura, K., Utani, A., Song, S.-Y., Otaka, A., Roller, P.P., Kleinman, H.K., and Yamada, Y. (1995) Identification of cell binding sites in the laminin α1 chain carboxyl-terminal globular domain by systematic screening of synthetic peptides. *J. Biol. Chem.* **270**, 20583-20590
16. Colognato-Pyke, H., O'Rear, J.J., Yamada, Y., Carbonetto, S., Chen, Y.-S., and Yurchenco, P.D. (1995) Mapping of network-forming, heparin binding, and α1β1 integrin-recognition sites

within the α-chain short arm of laminin-1. *J. Biol. Chem.* **270**, 9378-9406
17. Sasaki, M. and Yamada, Y. (1987) The laminin B2 chain has a multidomain homologous to the B1 chain. *J. Biol. Chem.* **262**, 17111-17117
18. Sasaki, M., Kato, S., Kohno, K., Martin, G.R., and Yamada, Y. (1987) Sequence of the cDNA encoding the laminin B1 chain reveals a multidomain protein containing cysteine-rich repeats. *Proc. Natl. Acad. Sci. USA* **84**, 935-939
19. Sasaki, M., Kleinman, H.K., Huber, H., Deutzmann, R., and Yamada, Y. (1988) Laminin, a multi-domain protein: the A chain has a unique domain and homology with the basement membrane proteoglycan and laminin B chains. *J. Biol. Chem.* **263**, 16536-16544
20. Beck, K., Dixon, T.W., Engel, J., and Parry, D.A.D. (1993) Ionic interaction in the coiled-coil domain of laminin determine the specificity of chain assembly. *J. Mol. Biol.* **31**, 311-323
21. Kammerer, R.A., Antonsson, P., Schulthess, T., Fauser, C., and Engel, J. (1995) Selective chain recognition in the C-terminal α-helical coiled-coil region of laminin. *J. Mol. Biol.* **250**, 64-73
22. Antonsson, P., Kammerer, R.A., Schulthess, T., Hänisch, G., and Engel, J. (1995) Stabilization of the α-helical coiled-coil domain in laminin by C-terminal disulfide bonds. *J. Mol. Biol.* **250**, 74-79
23. Engvall, E. (1993) Laminin variants: why, where, and when? *Kidney Int.* **43**, 2-6
24. Tryggvason, K. (1993) The laminin family. *Curr. Opin. Cell Biol.* **5**, 877-882
25. Timpl, R. and Brown, J.D. (1994) The laminins. *Matrix Biol.* **14**, 275-281
26. Iivanainen, A., Sainio, K., Sariola, H., and Tryggvason, K. (1995) Primary structure and expression of a novel human laminin α4 chain. *FEBS Lett.* **365**, 183-188
27. Miner, J.H., Lewis, R.M., and Sanes, J.R. (1995) Molecular cloning of a novel laminin chain, α5, and widespread expression in adult mouse tissues. *J. Biol. Chem.* **270**, 28523-28526
28. Ehrig, K., Leivo, I., Argraves, W.S., Ruoslahti, E., and Engvall, E. (1990) Merosin, a tissue specific basement membrane protein is a laminin-like protein. *Proc. Natl. Acad. Sci. USA* **87**, 3264-3268
29. Marinkovich, M.P., Lunstrum, G.P., Keene, D.R., and Burgeson, R.E. (1992) The dermal-epidermal junction of human skin contains a novel laminin variant. *J. Cell Biol.* **119**, 695-703
30. Vuolteenaho, R., Nissinen, M., Sainio, K., Byers, M., Eddy, R., Hirvonen, H., Shows, T.B., Sariola, H., Engvall, E., and Tryggvason, K. (1994) Human laminin M chain (merosin): complete primary structure, chromosomal assignment, and expression of the M and A chain in human fetal tissues. *J. Cell Biol.* **124**, 381-394
31. Hunter, D.D., Shah, V., Merlie, J.P., and Sanes, J.R. (1989) A laminin-like adhesive protein concentrated in the synaptic cleft of the neuromuscular junction. *Nature* **338**, 229-234
32. Rousselle, P., Lunstrum, G.P., Keene, D.R., and Burgeson, R.E. (1991) Kalinin: an epithelium-specific basement membrane adhesion molecule that is a component of anchoring filaments. *J. Cell Biol.* **114**, 567-576
33. Kallunki, P., Sainio, K., Eddy, R., Byers, M., Kallunki, T., Sariola, H., Beck, K., Hirvonen, H., Shows, T.B., and Tryggavason, K. (1992) A truncated laminin chain homologous to the B2 chain: structure, spatial expression, and chromosomal assignment. *J. Cell Biol.* **119**, 679-693
34. Aratani, Y. and Kitagawa, Y. (1988) Enhanced synthesis and secretion of type IV collagen and entactin during adipose conversion of 3T3-L1 cells and production of unorthodox laminin complex. *J. Biol. Chem.* **263**, 16163-16169
35. Tokida, Y., Aratani, Y., Morita, A., and Kitagawa, Y. (1990) Production of two variant laminin forms by endothelial cells and shift of their relative levels by angiostatic steroids. *J. Biol. Chem.* **265**, 18123-18129
36. Hunter, I., Schulthess, T., Bruch, M., Beck, K., and Engel, J. (1990) Evidence for a specific mechanism of laminin assembly. *Eur. J. Biochem.* **188**, 205-211
37. Hunter, I., Schulthess, T., and Engel, J. (1992) Laminin chain assembly by triple and double stranded coiled-coil structures. *J. Biol. Chem.* **267**, 6006-6011
38. Utani, A., Nomizu, M., Timpl, R., Roller, P.P., and Yamada, Y. (1994) Laminin chain assembly. Specific sequences at the C terminus of the long arm are required for the formation of specific double- and triple stranded coiled-coil structures. *J. Biol. Chem.* **269**, 19167-19175
39. Utani, A., Nomizu, M., Sugiyama, S., Miyamoto, S., Roller, P.P., and Yamada, Y. (1995) A specific sequence of the laminin α2 chain critical for the initiation of heterotrimer assembly. *J. Biol. Chem.* **270**, 3292-3298
40. Nomizu, M., Otaka, A., Utani, A., Roller, P.P., and Yamada, Y. (1994) Assembly of synthetic laminin peptides into a triple-stranded coiled-coil structure. *J. Biol. Chem.* **269**, 30386-30392
41. Nomizu, M., Utani, A., Beck, K., Otaka, A., Utani, A., Roller, P.P., and Yamada, Y. (1996) Mechanism of laminin chain assembly into a triple-stranded coiled-coil structure. *Biochemistry* **35**, 2885-2893
42. Ohashi, H., Maruyama, K., Liu, Y.-C., and Yoshimura, A. (1994) Ligand-induced activation of chimeric receptors between the erythropoietin receptor and receptor tyrosine kinases. *Proc. Natl. Acad. Sci. USA* **91**, 158-162
43. Egan, E.S., Giddings, B.W., Brooks, M.W., Buday, L., Sizeland, A.M., and Weinberg, R.A. (1993) Association of Sos Ras exchange protein with Grb2 is implicated in tyrosine kinase signal transduction and transformation. *Nature* **363**, 45-51
44. Miki, K., Sugimoto, E., and Kitagawa, Y. (1987) Reversible interconversion between primitive endoderm- and parietal endoderm-like F9 cells demonstrated by mRNAs expression. *J. Biochem.* **102**, 385-392
45. Martin, G.R., Wiley, L.M., and Damjanov, I. (1977) The development of cystic embryoid bodies *in vitro* from clonal teratocarcinoma stem cells. *Dev. Biol.* **61**, 230-244
46. Graham, F.L. and van der Eb, A.J. (1973) A new technique for the assay of infectivity of human adenovirus IV DNA. *Virology* **52**, 456-467
47. Morita, A., Sugimoto, E., and Kitagawa, Y. (1985) Post-translational assembly and glycosylation of laminin subunits in parietal endoderm-like F9 cells. *Biochem. J.* **229**, 259-264
48. Engvall, E. and Wewer, U.M. (1996) Domains of laminin. *J. Cell Biochem.* **61**, 493-501